
GNNS, YOU CAN BE STRONGER, DEEPER AND FASTER

Jingbo Zhou^{1,4,*}, Yixuan Du^{1,4,*}, Ruqiong Zhang^{1,4,*}, Rui Zhang^{1,4,†}, Di Jin², and Carl Yang³

¹College of Computer Science and Technology, Jilin University, China

²Collage of Intelligence of Computing, Tianjin University, China

³Department of Computer Science, Emory University, USA

⁴Key Laboratory of Symbolic Computation and Knowledge Engineering of Ministry of Education, China

ABSTRACT

Graph neural networks (GNNs), a type of neural network that can learn from graph-structured data and learn the representation of nodes by aggregating their neighbors, have shown excellent performance in downstream tasks. However, it is known that the performance of graph neural networks (GNNs) degrades gradually as the number of layers increases. Based on k-hop subgraph aggregation, which is a new concept, we propose a new perspective to understand the expressive power of GNN. From this perspective, we reveal the potential causes of the performance degradation of the deep traditional GNN - aggregated subgraph overlap, and the fact that the residual-based graph neural networks in fact exploit the aggregation results of 1 to k hop subgraphs to improve the effectiveness. Further, we propose a new sampling-based node-level residual module named SDF, which is shown by theoretical derivation to obtain a superior expressive power compared to previous residual methods by using information from 1 to k hop subgraphs more flexibly. Extensive experiments show that the performance and efficiency of GNN with the SDF module outperform other methods. Our code is publicly available at <https://github.com/JingboZhou-JLU/SDF-GNN>.

Keywords Graph Neural Networks · Graph Representation Learning

1 INTRODUCTION

In recent years, GNNs have become the state of the art model for processing graph-structured data and are widely used in various fields such as social networks[1], recommender systems[2], and drug discovery[3]. Through the message passing mechanism that aggregates representation of neighboring nodes, GNNs provide a general framework for learning from graph-structured data.

Despite great success, according to previous studies[4, 5], GNNs show significant performance degradation as the number of layers increases, which prevents GNNs from going deeper to utilize multi-hop neighborhood structures to better learn node representation.

The main reason for this situation is now widely believed to be over-smoothing[6, 7, 5, 8]. However, since ResNet[9] solved a similar problem in computer vision with residual connection, several new works have been inspired to apply the idea of residual connection to GNNs to alleviate the over-smoothing phenomenon in graph neural networks and thus improve the expressive power of the models. For example, JKNet[5] learns node representations by aggregating the outputs of all previous layers at the last layer; DenseGCN[10] concatenates the results of the current layer and all previous layers as the node representation of this layer; APPNP[8] uses initial residual connection to retain the initial feature information with probability α , and utilizes the feature information aggregated at the current layer with probability $1 - \alpha$.

In this paper, we propose a new understanding perspective on message-passing GNNs, called k-hop subgraph aggregation. Based on this perspective, we show that the single higher-hop subgraph aggregation of traditional GNNs is limited by their corresponding k-hop subgraphs that are prone to information overlap, which makes the node representation obtained from k-hop subgraph aggregation indistinguishable, i.e., over-smoothing occurs, which in turn leads to

performance degradation of deep GNNs. Through theoretical analysis, we further show that the existing k-layer residual-based GNN model actually utilizes 1 to k hop subgraph aggregations in a different way to improve expressive power.

After understanding GNNs from the perspective of k-hop subgraph and experimentally verifying the existence of subgraph information overlap, we aim to adequately and flexibly exploit the information of 1 to k hop subgraphs by designing a new residual module to enhance GNN expressive power. In particular, we propose a generic sampling-based node-level residual module named SDF. Compared with traditional GNNs that can only learn information from a single k-hop subgraph, which may have more information overlap, proposed SDF module use information from 1 to k hop subgraphs efficiently and flexibly based on the sampled learnable coefficients, thus significantly improving the performance of GNNs. A theoretical proof of this is provided in the paper. Our contribution can be summarized as follows:

1. **We propose a new perspective to understand the expressive power of message-passing GNNs, which we call k-hop subgraph aggregation theory. Based on this perspective, we analyze the reason why the performance of GNN degrades as the number of layers increases and give experimental verification. In addition, we provide a theoretical analysis of the expressive power of different previous GNN variant models based on residual connection and prove that they are in fact different forms of integration of the information from 1 to k hop subgraphs.**
2. **We propose a new generic sampling-based residual module SDF and demonstrate through theoretical derivation that this module can more flexibly and adequately utilize the information of 1 to k hop subgraphs to improve the performance of GNNs.**
3. **Extensive experiments showing that GNNs using proposed SDF module achieve better performance than other methods, as well as with higher training efficiency, on semi-supervised tasks as well as on tasks requiring deep GNNs.**

2 BACKGROUND and RELATED WORK

2.1 Notations

A connected undirected graph is represented by $\mathcal{G} = (\mathcal{V}, \mathcal{E})$, where $\mathcal{V} = \{v_1, v_2, \dots, v_N\}$ is the set of N nodes, $\mathcal{E} \subseteq \mathcal{V} \times \mathcal{V}$ is the set of edges. $\mathbf{H} \in \mathbb{R}^{N \times d}$ indicates the node feature matrix with d as the length of feature. Let $\mathbf{A} \in \{0, 1\}^{N \times N}$ denote the adjacency matrix where $\mathbf{A}_{ij} = 1$ indicates the existence of an edge between nodes v_i and v_j . The node degrees are given by the degree matrix \mathbf{D} whose elements d_i computes the number of edge connected to node v_i . $\tilde{\mathbf{A}} = \mathbf{A} + \mathbf{I}$ is the adjacency matrix with self loop and correspondingly $\tilde{\mathbf{D}} = \mathbf{D} + \mathbf{I}$.

2.2 Graph Neural Networks

A graph neural network consists of several GNN layers, where each layer updates the representation of each node via aggregating itself and its neighbors' representations following the message passing strategy[11]. Specifically, a layer's input is a set of node representations $\{\mathbf{h}_i \in \mathbb{R}^d \mid i \in \mathcal{V}\}$ and the output is a new set of node representations $\{\mathbf{h}'_i \in \mathbb{R}^{d'} \mid i \in \mathcal{V}\}$ computed as:

$$\mathbf{h}'_i = \mathbf{f}_\theta(\mathbf{h}_i, \text{AGGREGATE}(\{\mathbf{h}_j \mid j \in \mathcal{N}_i\}))$$

where the **AGGREGATE** function is applied to its neighbors given by $\mathcal{N}_i = \{j \in \mathcal{V} \mid (j, i) \in \mathcal{E}\}$, and the parametric function \mathbf{f}_θ denotes the update function with \mathbf{h}_i and the output of the **AGGREGATE** function as input. The key to the performance of different GNNs is in the design of the \mathbf{f}_θ and **AGGREGATE** function.

2.2.1 Graph Convolutional Networks

GCN is originally proposed by Kipf & Welling (2017)[12]. A multi-layer Graph Convolutional Network (GCN) follows layer-wise propagation rule:

$$\mathbf{H}^{(l+1)} = \sigma \left(\tilde{\mathbf{D}}^{-\frac{1}{2}} \tilde{\mathbf{A}} \tilde{\mathbf{D}}^{-\frac{1}{2}} \mathbf{H}^{(l)} \mathbf{W}^{(l)} \right)$$

where $\mathbf{H}^{(l+1)} = \{\mathbf{h}_1^{(l+1)}, \dots, \mathbf{h}_N^{(l+1)}\}$ are the feature matrix of the l^{th} layer with $\mathbf{h}_i^{(l)}$ as the representation for node v_i at layer l ; $\mathbf{W}^{(l)}$ is a layer-specific learnable weight matrix; $\sigma(\cdot)$ denotes an activation function.

2.2.2 Graph Attention Networks

Petar Velickovic & Guillem Cucurull (2017)[13] introduce self attention mechanism to graph neural network. The normalized attention coefficient equation is defined as follows:

$$\alpha_{ij} = \frac{\exp \left(\text{LeakyReLU} \left(\vec{\mathbf{a}}^T [\mathbf{W}\vec{\mathbf{h}}_i \parallel \mathbf{W}\vec{\mathbf{h}}_j] \right) \right)}{\sum_{k \in \mathcal{N}_i} \exp \left(\text{LeakyReLU} \left(\vec{\mathbf{a}}^T [\mathbf{W}\vec{\mathbf{h}}_i \parallel \mathbf{W}\vec{\mathbf{h}}_k] \right) \right)}$$

where \cdot^T represents transposition and \parallel is the concatenation operation.

Once obtained, GAT use the attention coefficients to compute a linear combination of the features corresponding to them, to serve as the final output feature for each node:

$$\vec{\mathbf{h}}'_i = \sigma \left(\sum_{j \in \mathcal{N}_i} \alpha_{ij} \mathbf{W}\vec{\mathbf{h}}_j \right).$$

2.3 Residual Connection

Several new works have used residual connection to solve the problem of over-smoothing. Common residual connection for GNNs and their corresponding GNNs are described below.

2.3.1 ResNet

ResNet[9] is composed of multiple residual blocks containing few stacked layers. Taking the initial input of the n -th residual block as \mathbf{X}_n , and the stacked nonlinear layers within the residual block as $\mathbf{F}(\mathbf{X})$:

$$\mathbf{X}_{n+1} = \mathbf{F}(\mathbf{X}_n) + \mathbf{X}_n$$

where identity mapping and residual mapping refer to \mathbf{X} and $\mathbf{F}(\mathbf{X})$ on the left side of the above equation, respectively. Inspired by ResNet, Guohao Li & Matthias Müller(2019)[10] proposed a residual connection learning framework for GCN and called this model ResGCN.

2.3.2 Initial ResNet

The initial residual connection is proposed for the first time in APPNP[8], unlike the residual connection that carries information from the previous layer, it constructs a connection to the initial representation \mathbf{X}_0 at each layer:

$$\mathbf{X}_{n+1} = (1 - \alpha)\mathbf{H}(\mathbf{X}_n) + \alpha\mathbf{X}_0$$

where $\mathbf{H}(\mathbf{X})$ denotes the aggregation operation within one layer. The initial residual connection ensures that even after stacking many layers, the final representation of each node retains at least α -size of the initial feature information. Considering the overfitting problem, APPNP uses a linear combination between different layers, and thus remains a shallow model. Based on APPNP, GCNII[14] borrows the idea of identity mapping from ResNet to make up for the deficiency in APPNP.

2.3.3 DenseNet

DenseNet[15] proposes a more efficient way to reuse features between layers. The input of each layer of the network includes the outputs of all previous layers of the network and stitches them together:

$$\mathbf{X}_{n+1} = \mathbf{H}([\mathbf{X}_0, \mathbf{X}_1, \dots, \mathbf{X}_n])$$

where $[\cdot]$ denotes the concatenation of the feature map for the output of layers 0 to n . Inspired by DenseNet, DenseGCN[10] applies a similar idea to GCN, i.e., let the output of the n -th layer contains transformations from all previous GCN layers to exploit the flow of information from different GCN layers.

2.3.4 Jump Connection

The first deep GCN framework is proposed by (Xu et al., 2018)[5]. At the last layer, JKNet sifts from all previous representations $[\mathbf{X}_1, \dots, \mathbf{X}_K]$ and combines them to learn representations of different orders for different graph substructures:

$$\mathbf{X}_{output} = \mathcal{AGG}(\mathbf{X}_1, \dots, \mathbf{X}_K)$$

The \mathcal{AGG} operation include concatenation, Maxpooling and LSTM-attention.

3 PRELIMINARY STUDY

3.1 K-hop Subgraph Information Analysis on GNNs

Message-passing GNNs recursively update the features of each node by aggregating information from its neighbors, allowing them to capture both the graph topology and node features. In the examples presented below, we use GCN as a representative model. Additionally, we assume that the feature matrix \mathbf{H} is non-negative, which allows us to simplify the model by removing the elu activation function and ignoring the weight matrix.

We define a k -hop subgraph associated with a specific node as the subgraph consisting of nodes from which the node can aggregate information after k rounds of message passing. In the case of GCN, each aggregation operation is based on the previous aggregation, allowing us to consider the result of a node obtained after k layers of GCN aggregation as equivalent to the aggregation in a k -hop subgraph associated with it.

The figure 1 shows that, after two aggregation operations, nodes on layer 2 obtain 1-hop neighbor and 2-hop neighbor information in layer 0, respectively. According to the definition of the k -hop subgraph, the information of the node on layer 2 in the figure is composed of all reachable nodes information shown on layer 0. Furthermore, for the entire graph,

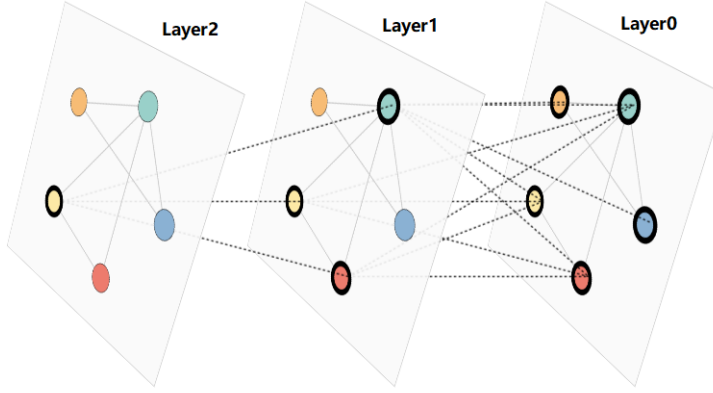


Figure 1: K-hop subgraph.

since the GCN performs k graph convolution operations on the k -hop subgraph, we can represent the aggregation of the k -hop subgraph as follows:

$$\mathbf{H}_k = \mathbf{N}^k \mathbf{H} \quad (1)$$

where \mathbf{N} denotes $\tilde{\mathbf{D}}^{-\frac{1}{2}} \tilde{\mathbf{A}} \tilde{\mathbf{D}}^{-\frac{1}{2}}$.

3.2 A New Perspective Views Over-smoothing

It is evident that as the number of aggregation operations increases, the reachable information range of a node expands rapidly. Specifically, the size of its k -hop subgraph grows exponentially as k increases, leading to a significant increase in overlap between the k -hop subgraphs of different nodes. As a result, the aggregation result of different nodes on their respective k -hop subgraphs becomes indistinguishable.

Furthermore, in a specific graph dataset, nodes with higher degrees tend to have a larger range of k -hop subgraphs compared to nodes with lower degrees. As a result, the subgraphs are more likely to overlap between nodes with higher degrees, making their aggregation results more likely to become similar and indistinguishable.

To verify this point, we conducted experiments on three graph datasets, Cora, Citeseer, and Pubmed. First, we grouped the nodes according to their degrees by assigning nodes with degrees in the range $[2^i, 2^{i+1})$ to the i -th group. Subsequently, we performed aggregation with different layers of Graph Convolutional Networks (GCN) and Graph Attention Networks (GAT). We calculated the degree of smoothing of the node representation within each group separately for different groups of nodes. We used the metric proposed in [] to measure the smoothness of the node representation within each group, namely **SMV**, which calculates the average of the distances between the nodes within the group.

$$\text{SMV}(\mathbf{X}) = \frac{1}{N(N-1)} \sum_{i \neq j} \mathbf{D}(\mathbf{X}_{i,:}, \mathbf{X}_{j,:}) \quad (2)$$

where $\mathbf{D}(\cdot, \cdot)$ is the normalized Euclidean distance between the two vectors:

$$\mathbf{D}(\mathbf{x}, \mathbf{y}) = \frac{1}{2} \left\| \frac{\mathbf{x}}{\|\mathbf{x}\|} - \frac{\mathbf{y}}{\|\mathbf{y}\|} \right\|_2 \quad (3)$$

By definition, a smaller value of **SMV** indicates a greater similarity in node representations.

We selected the most representative results, as illustrated in the Figure 2.

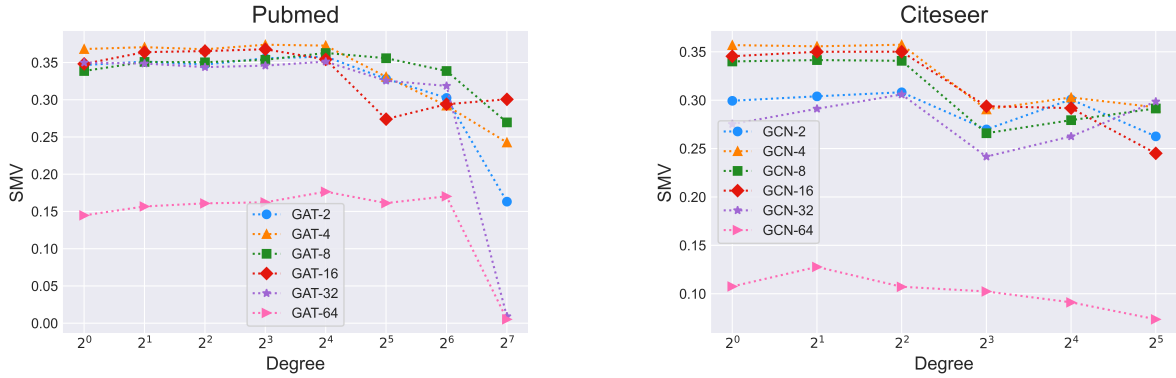


Figure 2: SMV of varying degrees nodes

As shown in Figure 2, it can be seen that the groups of nodes with higher degree tend to be more likely to have high similarity in the representation of nodes within the group in different layers of the model. This finding supports our claim.

After obtaining this conclusion, revisiting traditional k-layer graph neural networks (GNNs), we find that they only use the aggregated results of the k-hop subgraphs, making them prone to over-smoothing. Therefore, a model that fully utilizes the aggregated information of 1 to k hop subgraphs can alleviate the problem of indistinguishable representations caused by subgraph overlap and, subsequently, the over-smoothing phenomenon. In the following section, we will demonstrate that the previous k-layer residual-based graph neural network models are actually different forms of integration of aggregation results of 1 to k hop subgraphs.

3.3 Revisiting Previous Models in a New Perspective

Based on our settings in 3.1, we next revisit the previous model's treatment of multiple k-hop subgraph aggregation. Details of the derivation of the theorems in this part are given in the Appendix.

3.3.1 ResGCN

The equation for ResGCN can be written as :

$$\mathbf{H}_k = \mathbf{H}_{k-1} + \mathbf{N}\mathbf{H}_{k-1} \quad (4)$$

We can derive its general term of ResGCN:

Theorem 1. *The general term of ResGCN is : $\mathbf{H}_k = \sum_{j=0}^k \mathbf{C}_k^j \mathbf{N}^j \mathbf{H}$*

The following result can be obtained from the generic formula: the result of k-layer ResGCN contains all 0 to K hop subgraph aggregation .

3.3.2 APPNP

The equation for APPNP can be written as :

$$\mathbf{H}_k = (1 - \alpha) \mathbf{N} \mathbf{H}_{k-1} + \alpha \mathbf{H} \quad (5)$$

We can derive its general term of APPNP:

$$\text{Theorem 2. } \text{The general term of APPNP is : } \mathbf{H}_k = ((1 - \alpha) \mathbf{N})^k \mathbf{H} + \alpha \sum_{j=0}^{k-1} \sum_{i=0}^j (-1)^{j-i} (1 - \alpha)^i \mathbf{N}^i \mathbf{H}$$

The following result can be obtained from the generic formula: the result of k-layer APPNP contains all 0 to k hop subgraph aggregation results, and The higher the i , the lower the percentage of $\mathbf{N}^i \mathbf{H}$ in the results. The first point guarantees the expressive power of APPNP to a certain extend, while the second point shows that the larger the k is, the less the k-hop subgraph aggregation on account for the output, which elucidates from another perspective that APPNP is still essentially a shallow model.

3.3.3 JKNet and DenseGCN

DenseGCN can be written in the following form at the k layer:

$$\mathbf{H}_1 = \mathbf{N} \mathbf{H}, \quad \mathbf{H}_k = \mathbf{AGG}_{dense}(\mathbf{H}, \mathbf{H}_1, \dots, \mathbf{H}_{k-1}) \quad (6)$$

While JKNet be written as :

$$\mathbf{H}_k = \mathbf{N} \mathbf{H}_{k-1}, \quad \mathbf{H}_{output} = \mathbf{AGG}_{jk}(\mathbf{N} \mathbf{H}, \dots, \mathbf{N}^{k-1} \mathbf{H}) \quad (7)$$

The \mathbf{AGG}_{dense} of DenseGCN is a densely fused vertex-wise cascading function, and the \mathbf{AGG}_{jk} of JKNet is concatenation, Maxpooling or LSTM-attention, and they can all be seen as a superposition or trade-off of 0 to k hop subgraph aggregation in some way at the last layer.

3.3.4 Discussion

From the above derivation, we can see that, in comparison to message-passing GNNs, residual-based variants of GNNs can utilize multiple k-hop subgraphs. There are two methods to exploit them: **(1) Summation, such as ResGCN and APPNP; (2) Aggregation functions, which use concatenation to leverage information from multiple k-hop subgraphs, such as DenseNet and JKNet.** The concept of residuals is derived from computer vision, where images are the fundamental unit for most computer vision tasks. However, in semi-supervised node classification, nodes are the fundamental unit. Therefore, the direct transfer of residuals to GNNs assumes that the information from the subgraph of the same hop are equally important for different nodes, which limits the expressive power of GNNs based on residual variants. This reveals the need for designing a node-level residual module that can more flexibly utilize information from multiple k-hop subgraphs for different nodes.

4 THE PROPOSED MODULE

4.1 Module Definition

We define SDF residual module as:

$$\mathbf{h}_{k-1}^{(i)'} = \mathbf{GraphConv}(\mathbf{h}_{k-1}^{(i)}) \quad (8)$$

$$\mathbf{h}_k^{(i)} = \mathbf{h}_1^{(i)} + \mathbf{p}_k^{(i)} \left(\mathbf{h}_1^{(i)} - \mathbf{h}_{k-1}^{(i)'} \right), \quad \mathbf{p}_k^{(i)} \sim \text{Sigmoid}(\mathcal{N}(\alpha_{k-1}^{(i)}, \beta_{k-1}^{(i)2})) \quad (9)$$

where $\mathbf{h}_k^{(i)}$ denotes the representation of k -th layer of node i ; $\mathbf{h}_k^{(i)'}$ denotes the result obtained by an arbitrary graph neural network layer with $\mathbf{h}_{k-1}^{(i)}$ as input ; $\mathbf{p}_k^{(i)}$ is a random number in the range $(0, 1)$ sampled from $\mathcal{N}(\alpha_{k-1}^{(i)}, \beta_{k-1}^{(i)2})$ which associated with the i -th node at the k -th layer and converted by sigmoid while $\alpha_{k-1}^{(i)}$ and $\beta_{k-1}^{(i)}$ are learnable parameters representing the standard deviation and mean of this distribution, respectively.

4.2 Analysis

4.2.1 Theoretical Analysis of Model Performance

We next analyze the expressive power of GCN with SDF module. First of all, Combined with the previous definition 9, the matrix form of the recurrence formula of the GCN model that introduces the SDF residual module can be written as:

$$\mathbf{H}_k = \mathbf{H}_1 + \Lambda_{k-1} \left(\mathbf{H}_1 - \tilde{\mathbf{D}}^{-1/2} \tilde{\mathbf{A}} \tilde{\mathbf{D}}^{-1/2} \mathbf{H}_{k-1} \right) \quad (10)$$

Combined with the previous discussion, the following will evaluate its expressive power by analyzing the utilization of a k-layer SDF-GCN for different 1 to k subgraph aggregations.

We first try to obtain the general term formula of SDF-GCN according to this recursive formula. We can prove the following theorem:

Theorem 3. *Given that $0 < \lambda_{k-1}^{(n)} < 1$, then the general term formula of SDF-GCN is: $\mathbf{H}_k = \sum_{i=2}^{k-1} \prod_{j=i}^{k-1} \tilde{\mathbf{N}}_j (\mathbf{M}_i - \mathbf{M}_{i-1}) + \prod_{i=1}^{k-1} \tilde{\mathbf{N}}_i (\mathbf{H}_1 + \mathbf{M}_1) - \mathbf{M}_{k-1}$ where $\tilde{\mathbf{N}}_i = -\Lambda_{k-1} \mathbf{N}$ and $\mathbf{M}_k = -(\Lambda_k \mathbf{N} + \mathbf{I})^{-1} (\mathbf{I} + \Lambda_k) \mathbf{H}_1$.*

From the general term formula of SDF-GCN, we can see that \mathbf{M}_k is a linear transformation of \mathbf{H}_1 , Therefore, the first two terms of the formula can be approximately regarded as a new form of subgraph aggregation. Further we can find that all 1 to k hop subgraph aggregations appear in the formula, which ensures the expressive power of our model. Furthermore, because Λ_k are learnable diagonal matrix, SDF-GCN's subgraph aggregation is more flexible and learnable, which further makes expressive power stronger.

Besides, when we set $\Lambda_k = -\alpha \mathbf{I}$, the first term will be 0, and the rest become APPNP, which means SDF-GCN can be approximately regarded as a more fine-grained expressive APPNP.

4.2.2 Motivation of SDF Module and the Introduction of Randomness

Another key point of SDF is that it introduced randomness to alleviate overfitting. In our original idea, we attempted to build a generic module similar to the initial residual at the node level. Based on this, we initially designed the following modules:

$$\mathbf{h}_k^{(i)} = \mathbf{h}_1^{(i)} - \sigma \left(\mathbf{p}_k^{(i)} \right) \left(\mathbf{h}_1^{(i)} - \mathbf{h}_{k-1}^{(i)} \right)'$$

where $\mathbf{p}_k^{(i)}$ is a learnable parameter which associated with the i-th node at the k-th layer. After conducting experiments, we discovered that the model has a high risk of overfitting when adding this module, particularly with a high number of layers. However, we also found that this issue can be resolved by learning a distribution related to it and randomly sampling during each computation, rather than directly learning all p through the backpropagation gradient. This modification significantly improved the performance of the model, leading us to modify the module as follows:

$$\mathbf{h}_k^{(i)} = \mathbf{h}_1^{(i)} - \mathbf{p}_k^{(i)} \left(\mathbf{h}_1^{(i)} - \mathbf{h}_{k-1}^{(i)} \right)', \quad \mathbf{p}_k^{(i)} \sim \text{Sigmoid}(\mathcal{N}(\alpha_{k-1}^{(i)}, \beta_{k-1}^{(i)}))$$

It is worth noting that GCNII and SDF-GCN share a similar architecture that can be approximated as a more fine-grained APPNP-like model. However, when faced with the problem of overfitting due to their high number of parameters, GCNII added an identity matrix to mitigate the issue. Subsequent experiments have shown that SDF-GCN's learning distribution-sampling approach is more effective in mitigating overfitting.

5 EXPERIMENT

In this section, we aim to experimentally evaluate the effectiveness of SDF on real datasets. To achieve this, we will compare the performance of SDF with other methods and answer the following research questions: **Q1: How effective is SDF on classical tasks that prefer shallow models?** **Q2: Can SDF help overcome the over-smoothing problem in GNNs and enable training of deeper models?** **Q3: How effective is SDF on tasks that require deep GNNs?** **Q4: How efficient is the training of SDF?**

5.1 Experiment Setup

In our study, we conducted experiments on four tasks: semi-supervised node classification, semi-supervised node classification with missing vectors, alleviating performance drop in deeper GNNs, and efficiency evaluation. These tasks are referred to by their respective abbreviations throughout the paper.

To assess the effectiveness of our proposed framework, we utilized five widely-used benchmark datasets within the GNN domain, including Cora, Citeseer, Pubmed (Sen et al., 2008)[16], CoauthorCS (Shchur et al., 2018)[17], and CoraFull for testing purposes. Details on the characteristics of these datasets and the specific data splitting procedures used can be found in Appendix A.7.

We considered two fundamental GNN models, GCN[12] and GAT[13], and equipped them with the following residual modules: Res, InitialRes, Dense, JK, and SDF. For GCN, we tested its residual variant models, including ResGCN[10], APPNP[8], DenseGCN[10], GCNII[14] and JKNet[5]. For GAT, we directly tested the addition of residual modules. Additionally, for the SSNC-MV task, we compared our proposed models with several classical over-smoothing mitigation techniques, including BatchNorm[18], Pairnorm[19], DGN[20], Decorr[21], and DropEdge[22]. Further details on these models and techniques can be found in the following sections.

For all benchmark and variant models, the linear layers in the models were initialized with a standard normal distribution, and the convolutional layers were initialized with Xavier initialization. The Adam optimizer[23] was used for all models. Further details on the specific parameter settings used can be found in Appendix A.7.

All models and datasets used in this paper were implemented using the Deep Graph Library(DGL). All experiments are conducted on a server with 15 vCPU Intel(R) Xeon(R) Platinum 8358P CPU @ 2.60GHz, A40 with 48GB GPU memory, and 56GB main memory.

5.2 Semi-supervised Node Classification

To compare the performance of our proposed residual modules with those previously proposed for use with GCN, we applied four classic residual modules, DenseNet, ResNet, InitialResNet, and JKNet, to two fundamental GNN models, GCN and GAT. Our objective was to observe the performance improvements achieved by GCN and GAT using various residual modules.

To ensure a fair comparison, we used the optimal parameters specified in the original papers for APPNP[8], GCNII[14], and JKNet[5] models, while keeping the parameter settings for other variant and base models the same. We varied the number of layers within the range of {1, 2, 3, ..., 10} and ran each experiment 10 times to determine the optimal number of layers that achieved the best performance and report the average accuracy achieved.

We compared the best results achieved by each backbone and found that, as shown in Table 1, GNN models with the SDF module consistently achieved the best performance in most cases.

Table 1: Node classification accuracy (%) for five datasets.

Method	Cora	Citeseer	Pubmed	CoauthorCS	CoraFull
GCN	78.51	66.54	77.54	85.90	55.64
ResGCN	79.40	67.02	77.85	84.99	56.70
APPNP	80.61	72.55	74.25	85.99	24.48
GCNII	72.36	65.66	71.74	85.47	50.70
DenseGCN	76.83	64.37	76.37	83.86	50.68
JKNet	77.64	62.38	78.20	83.17	52.91
SDF-GCN	81.80	69.22	77.47	86.12	57.65
GAT	77.66	66.54	77.35	80.22	53.09
Res-GAT	78.34	67.28	77.20	81.37	55.64
InitialRes-GAT	77.81	66.17	77.43	80.74	53.15
Dense-GAT	77.54	64.07	75.44	80.87	51.95
JK-GAT	77.81	64.41	77.50	79.99	55.09
SDF-GAT	79.47	69.15	77.51	82.81	56.24

However, as observed from the experimental results, many models with residual modules did not perform as well as expected, and in some cases, even showed reduced accuracy compared to the base models. According to previous research[19], we speculate that overfitting may have contributed to this phenomenon. To verify our hypothesis, we

conducted further experiments. Given that most models in the previous experiments achieved their best performance with shallow models, we selected models with two layers, trained them for 500 epochs, and recorded their accuracy on the training and validation sets at each epoch. Figure 3 shows the results on the training set.

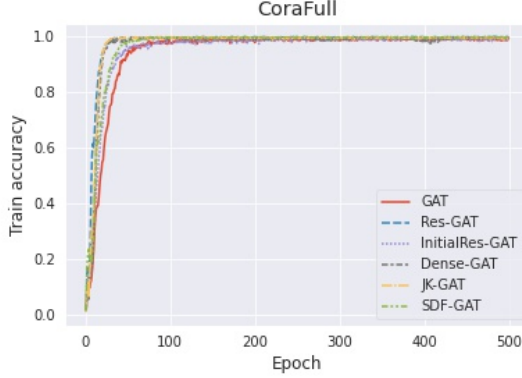


Figure 3: Train accuracy on CoraFull

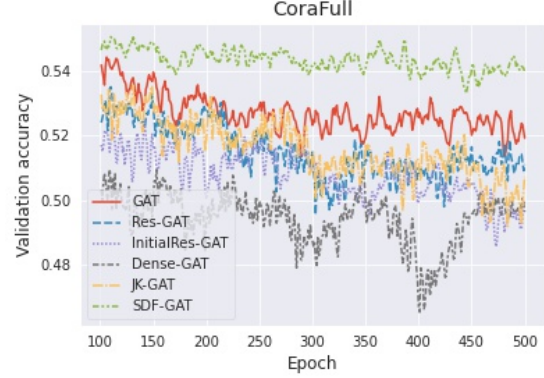


Figure 4: Validation accuracy on CoraFull

Most models showed signs of overfitting. To investigate this further, we observed the accuracy of the models on the validation set between epochs 100 and 500, when the models had already converged. As shown in Figure 4, the SDF module demonstrated the best ability to alleviate overfitting. Specifically, in shallow GNNs with limited subgraph aggregation, most models have similar expressive abilities, and overfitting is the main factor affecting their performance. Our proposed method effectively alleviates overfitting by learning a more representative distribution, resulting in better performance than the base models.

5.3 Alleviating Performance Drop in Deeper GNNs

As the number of layers in GNNs increases, over-smoothing occurs, resulting in decreased performance. Our objective is to investigate the performance of deep GNNs equipped with SDF and observe the impact of over-smoothing on their performance.

Table 2: Node classification accuracy (%) on different number of layers.

Dataset	Method	GCN			GAT		
		L2	L16	L32	L2	L16	L32
Cora	None	80.84	60.98	22.40	77.66	71.50	23.06
	Res	79.00	75.06	27.09	78.08	23.06	28.76
	InitialRes	77.72	66.22	69.02	77.46	72.64	16.20
	Dense	73.62	74.52	74.14	74.44	74.52	75.62
	JK	75.60	72.00	74.32	76.22	75.86	24.68
	SDF	81.34	79.20	78.10	78.84	79.28	79.60
Citeseer	None	65.54	42.18	18.96	68.80	51.02	22.90
	Res	67.34	62.72	24.12	66.92	24.16	24.48
	InitialRes	67.36	58.52	63.22	68.30	51.94	23.18
	Dense	63.04	59.48	57.56	65.10	60.60	60.78
	JK	62.72	55.06	57.70	66.38	60.68	23.06
	SDF	69.04	67.86	68.82	69.36	67.30	68.26
Pubmed	None	77.76	72.78	47.16	77.02	77.34	45.76
	Res	76.66	77.58	51.28	77.60	42.86	42.48
	InitialRes	75.24	71.52	68.40	76.94	77.90	47.18
	Dense	75.58	72.94	75.68	75.86	75.78	76.86
	JK	76.94	75.82	77.24	77.30	77.64	41.96
	SDF	78.62	77.88	77.66	77.70	77.92	77.58

We evaluated the performance of GNNs with different residual modules on 2, 16, and 32 layers using the Cora, Citeseer, and Pubmed datasets. The "None" column represents regular GNNs without any additional modules. The experimental results are presented in Table 2.

From Table 2, we can observe that GNNs consistently outperform other residual methods and the base models in all cases, given the same number of layers. SDF can significantly improve the performance of deep GNNs. For instance, on the Cora dataset, SDF improved the performance of 32-layer GCN and GAT models by **55.7%** and **56.54%**, respectively. By flexibly utilizing multiple subgraph aggregation results with our SDF module, we can enhance the expressive power of the model and produce more distinctive node representations than those of regular GNNs, thereby overcoming the over-smoothing problem. These results suggest that we can train deep GNN models based on SDF, making them suitable for tasks that require the use of deep GNNs.

5.4 Semi-supervised Node Classification with Missing Vectors

When do we need deep GNNs? [19] first proposed semi-supervised node classification with missing vectors (SSNC-MV), where all of a node's features are missing. Intuitively, more propagation steps, i.e., deeper GNNs, are needed to "recover" these nodes' effective feature representations. Modules that can maintain performance in deep layers would benefit more in this scenario.

SSNC-MV is a common and practical problem with various real-world applications. For example, new users on social networks often lack personal information[24]. To learn effective representations for these new users, we need more propagation of attribute information associated with existing users. Clearly, in this scenario, deeper GNNs can perform better than shallower ones. In fact, many graph-based classification tasks with cold-start problems can be transformed into SSNC-MV problems.

Table 3: Test accuracy (%) on missing feature setting.

Model	Method	Cora		Citeseer		Pubmed	
		Acc	#K	Acc	#K	Acc	#K
GCN	None	57.3	3	44.0	6	36.4	4
	BatchNorm	71.8	20	45.1	25	70.4	30
	PairNorm	65.6	20	43.6	25	63.1	30
	DGN	76.3	20	50.2	30	72.0	30
	DeCorr	73.8	20	49.1	30	73.3	15
	DropEdge	67.0	6	44.2	8	69.3	6
	ResGCN	74.9	9	58.4	7	76.6	10
	GCNII	59.0	1	48.2	1	69.9	1
	DenseGCN	70.8	15	56.1	8	75.3	8
	JKNet	71.8	10	56.7	7	75.9	6
GAT	SDF-GCN	77.1	10	62.9	20	76.6	8
	None	50.1	2	40.8	4	38.5	4
	BatchNorm	72.7	5	48.7	5	60.7	4
	PairNorm	68.8	8	50.3	6	63.2	20
	DGN	75.8	8	54.5	5	72.3	20
	DeCorr	72.8	15	46.5	6	72.4	15
	DropEdge	67.2	6	48.2	6	67.2	6
	Res	75.4	7	57.0	6	76.8	7
	InitialRes	72.9	4	56.2	7	77.1	7
	Dense	72.4	9	56.9	7	75.6	7
GAT	JK	73.3	8	56.9	7	77.0	7
	SDF-GAT	76.7	6	61.3	8	77.3	5

Previous research has shown that normalization techniques can be effective in mitigating over-smoothing and exploring deeper architectures. Therefore, we applied several classic normalization techniques and residual methods to GCN and GAT to compare their performance on tasks that require deep GNNs.

We removed the node features in the validation and test sets following the idea of SSNC-MV and took the same experimental settings as [19, 20, 21]. None, BatchNormN[18], PairNorm[19], DGN[20], DeCorr[21], and DropEdge[22] to reuse the experimental results reported by [21] on the three datasets. For all baseline models and variant models, the

results were obtained by applying the experimental settings in $\{1, 2, 3, \dots, 10, 15, \dots, 30\}$ varying the number of layers and running each layer five times, we select the layer that achieves the best performance and report its average accuracy. The results are reported in Table 3, where $\#K$ denotes the number of layers at which the model achieves the best performance. acc denotes the best test accuracy produced by the model equipped with the best number of layers $\#K$.

Our experiments showed that GNNs with the SDF module outperformed vanilla GNNs significantly in most cases. For instance, on the Pubmed dataset, SDF improved GCN and GAT by **40.2%** and **37.9%**, respectively. Additionally, we found that deeper models consistently achieved better performance; the optimal $\#K$ values for all models were relatively large. This suggests that more propagation steps are necessary to learn effective representations for nodes with missing features.

5.5 Efficiency Experiment

In real-world tasks, the rate at which a model achieves optimal performance through training is often important, and this affects the true effectiveness and time consumption of the model in real-world applications. To enable concrete measurement and comparison, here we define the following metrics for model training efficiency:

$$\text{Efficiency} = \frac{\text{Accuracy}}{\text{Time}}$$

where **Accuracy** denotes the accuracy of the model when it reaches its optimal performance and **Time** denotes the time when the model reaches its optimal performance. The definition of this formula shows that a larger **Efficiency** represents a higher performance per unit time improvement, and therefore a higher training efficiency.

Based on the above equation, we evaluated the training efficiency of the base GNNs model and the various types of residual modules. We used the 2, 4, 8, 16, 32, and 64-layer GNNs and their residual variants, respectively, and averaged five **Efficiency** calculated for each layer of the model. Specifically, each **Efficiency** was calculated based on the time for the model to reach the highest acc on the validation set after 100 epochs of training and the accuracy achieved on the test set at that time. The results are shown in Figure 5. The results on other datasets are shown in the Appendix A.7.

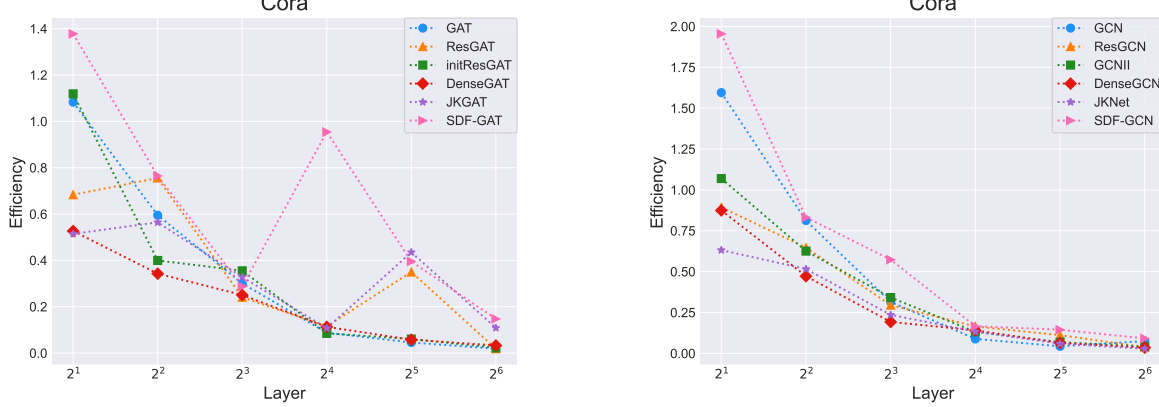


Figure 5: Efficiency

It can be noticed that the training efficiency of all models decreases as the number of layers increases, which is due to the increase in training time caused by the rise in the number of model parameters. However, in most cases, compared to other methods, our SDF module is able to maintain the highest training efficiency.

6 CONCLUSION

Our work proposes a new perspective for understanding the expressive power of GNNs: the k-hop subgraph aggregation theory. From this perspective, we have reinterpreted and experimentally validated the reason why the performance of classical GNNs decreases as the number of layers increases. Furthermore, we have evaluated the expressive power of previous residual-based GNN models based on this perspective. Building on these insights, we propose a new sampling-based generalized residual module SDF and show theoretically that SDF enables GNNs to more flexibly utilize information from multiple k-hop subgraphs, thus further improving the expressive power of GNNs. Extensive

experiments demonstrate that the proposed SDF can effectively address the issues of overfitting in shallow layers and oversmoothing in deep layers that are commonly encountered in traditional GNNs. As a result, the performance of GNNs is significantly improved, particularly SSNC-MV tasks. Our research will facilitate a deeper exploration of deep GNNs and enable a wider range of potential applications.

References

- [1] Bryan Perozzi, Rami Al-Rfou, and Steven Skiena. Deepwalk: Online learning of social representations. *CoRR*, abs/1403.6652, 2014.
- [2] Wenqi Fan, Yao Ma, Qing Li, Yuan He, Yihong Eric Zhao, Jiliang Tang, and Dawei Yin. Graph neural networks for social recommendation. *CoRR*, abs/1902.07243, 2019.
- [3] David Duvenaud, Dougal Maclaurin, Jorge Aguilera-Iparraguirre, Rafael Gómez-Bombarelli, Timothy Hirzel, Alán Aspuru-Guzik, and Ryan P. Adams. Convolutional networks on graphs for learning molecular fingerprints. *CoRR*, abs/1509.09292, 2015.
- [4] Qimai Li, Zhichao Han, and Xiao-Ming Wu. Deeper insights into graph convolutional networks for semi-supervised learning. *CoRR*, abs/1801.07606, 2018.
- [5] Keyulu Xu, Chengtao Li, Yonglong Tian, Tomohiro Sonobe, Ken-ichi Kawarabayashi, and Stefanie Jegelka. Representation learning on graphs with jumping knowledge networks. *CoRR*, abs/1806.03536, 2018.
- [6] Qimai Li, Zhichao Han, and Xiao-ming Wu. Deeper insights into graph convolutional networks for semi-supervised learning, 2018.
- [7] Kenta Oono and Taiji Suzuki. Graph neural networks exponentially lose expressive power for node classification, 2019.
- [8] Johannes Klicpera, Aleksandar Bojchevski, and Stephan Günnemann. Personalized embedding propagation: Combining neural networks on graphs with personalized pagerank. *CoRR*, abs/1810.05997, 2018.
- [9] Kaiming He, Xiangyu Zhang, Shaoqing Ren, and Jian Sun. Deep residual learning for image recognition. *CoRR*, abs/1512.03385, 2015.
- [10] Yulong Pei, Tianjin Huang, Werner van Ipenburg, and Mykola Pechenizkiy. Resgen: Attention-based deep residual modeling for anomaly detection on attributed networks. *CoRR*, abs/2009.14738, 2020.
- [11] Justin Gilmer, Samuel S. Schoenholz, Patrick F. Riley, Oriol Vinyals, and George E. Dahl. Neural message passing for quantum chemistry. *CoRR*, abs/1704.01212, 2017.
- [12] Thomas Kipf and M. Welling. Semi-supervised classification with graph convolutional networks. *International Conference on Learning Representations*, 2016.
- [13] Petar Veličković, Guillem Cucurull, Arantxa Casanova, Adriana Romero, P. Lio', and Yoshua Bengio. Graph attention networks. *International Conference on Learning Representations*, 2017.
- [14] Ming Chen, Zhewei Wei, Zengfeng Huang, Bolin Ding, and Yaliang Li. Simple and deep graph convolutional networks. *CoRR*, abs/2007.02133, 2020.
- [15] Gao Huang, Zhuang Liu, and Kilian Q. Weinberger. Densely connected convolutional networks. *CoRR*, abs/1608.06993, 2016.
- [16] Prithviraj Sen, Galileo Namata, Mustafa Bilgic, Lise Getoor, Brian Gallagher, and Tina Eliassi-Rad. Collective classification in network data. In *The AI Magazine*, 2008.
- [17] Oleksandr Shchur, Maximilian Mumme, Aleksandar Bojchevski, and Stephan Günnemann. Pitfalls of graph neural network evaluation. *CoRR*, abs/1811.05868, 2018.
- [18] Sergey Ioffe and Christian Szegedy. Batch normalization: Accelerating deep network training by reducing internal covariate shift. *CoRR*, abs/1502.03167, 2015.
- [19] Lingxiao Zhao and L. Akoglu. Pairnorm: Tackling oversmoothing in gnns. *International Conference on Learning Representations*, 2019.
- [20] Kaixiong Zhou, Xiao Huang, Yueling Li, D. Zha, Rui Chen, and Xia Hu. Towards deeper graph neural networks with differentiable group normalization. *Neural Information Processing Systems*, 2020.
- [21] Wei Jin, Xiaorui Liu, Yao Ma, Charu Aggarwal, and Jiliang Tang. Feature overcorrelation in deep graph neural networks. In *Proceedings of the 28th ACM SIGKDD Conference on Knowledge Discovery and Data Mining*. ACM, aug 2022.

- [22] Y. Rong, Wen-bing Huang, Tingyang Xu, and Junzhou Huang. Dropedge: Towards deep graph convolutional networks on node classification. *International Conference on Learning Representations*, 2019.
- [23] Diederik P. Kingma and Jimmy Ba. Adam: A method for stochastic optimization. *CoRR*, abs/1412.6980, 2014.
- [24] Al Mamunur Rashid, George Karypis, and John Riedl. Learning preferences of new users in recommender systems, 2008.

APPENDIX

A.1 Proof of theorem 1

We can derive its general term of ResGCN:

$$\mathbf{H}_k = (\mathbf{I} + \mathbf{N})\mathbf{H}_{k-1} \quad (11)$$

In turn, the following form can be obtained by recursion:

$$\mathbf{H}_k = (\mathbf{I} + \mathbf{N})^k \mathbf{H} \quad (12)$$

Using the binomial theorem can be written in the following form:

$$\mathbf{H}_k = \sum_{j=0}^k \mathbf{C}_k^j \mathbf{N}^j \mathbf{H} \quad (13)$$

A.2 Proof of theorem 2

Proof. According to the recurrence formula of APPNP:

$$\mathbf{H}_k = \alpha \mathbf{H} + (1 - \alpha) \mathbf{N} \mathbf{H}_{k-1},$$

To obtain the general formula, we can add a term \mathbf{T} to both ends of the equation at the same time:

$$\mathbf{H}_k + \mathbf{T} = (1 - \alpha) \mathbf{N} \mathbf{H}_{k-1} + \alpha \mathbf{H} + \mathbf{T}$$

We try to translate the equation into the following form:

$$\mathbf{H}_k + \mathbf{T} = (1 - \alpha) \mathbf{N} (\mathbf{H}_{k-1} + \mathbf{T}). \quad (14)$$

Then we need to make sure that there exists a very \mathbf{T} that satisfies the following equation:

$$(1 - \alpha) \mathbf{N} \mathbf{T} = \alpha \mathbf{H} + \mathbf{T},$$

which can be transformed into the following form:

$$((1 - \alpha) \mathbf{N} - \mathbf{I}) \mathbf{T} = \alpha \mathbf{H}.$$

We can proof that the following lemma:

Lemma 1. *Given that $\alpha \in (0, 1)$, $(1 - \alpha) \mathbf{N} - \mathbf{I}$ is invertible.*

Proof. To prove that $(1 - \alpha) \mathbf{N} - \mathbf{I}$ is invertible is equivalent to proving it does not have an eigenvalue of 0. Consider the Rayleigh quotient of $(1 - \alpha) \mathbf{N} - \mathbf{I}$:

$$\frac{\mathbf{X}^T ((1 - \alpha) \mathbf{N} - \mathbf{I}) \mathbf{X}}{\mathbf{X}^T \mathbf{X}} = (1 - \alpha) \frac{\mathbf{X}^T (\tilde{\mathbf{D}}^{-\frac{1}{2}} \tilde{\mathbf{A}} \tilde{\mathbf{D}}^{-\frac{1}{2}}) \mathbf{X}}{\mathbf{X}^T \mathbf{X}} - 1 \quad (15)$$

From spectral graph theory ,We can know the following equation holds:

$$\mathbf{X}^T (\tilde{\mathbf{D}}^{-\frac{1}{2}} \mathbf{L} \tilde{\mathbf{D}}^{-\frac{1}{2}}) \mathbf{X} = \sum_{(v_i, v_j) \in \mathcal{E}} \left(\frac{\mathbf{X}_i}{\sqrt{d_i + 1}} - \frac{\mathbf{X}_j}{\sqrt{d_j + 1}} \right)^2 > 0.$$

We can decompose \mathbf{L} into $\tilde{\mathbf{D}} - \tilde{\mathbf{A}}$, then we have:

$$\frac{\mathbf{X}^T (\tilde{\mathbf{D}}^{-\frac{1}{2}} \tilde{\mathbf{D}} \tilde{\mathbf{D}}^{-\frac{1}{2}}) \mathbf{X}}{\mathbf{X}^T \mathbf{X}} - \frac{\mathbf{X}^T (\tilde{\mathbf{D}}^{-\frac{1}{2}} \tilde{\mathbf{A}} \tilde{\mathbf{D}}^{-\frac{1}{2}}) \mathbf{X}}{\mathbf{X}^T \mathbf{X}} > 0$$

which is equivalent to :

$$\frac{\mathbf{X}^T (\tilde{\mathbf{D}}^{-\frac{1}{2}} \tilde{\mathbf{A}} \tilde{\mathbf{D}}^{-\frac{1}{2}}) \mathbf{X}}{\mathbf{X}^T \mathbf{X}} < \frac{\mathbf{X}^T \mathbf{I} \mathbf{X}}{\mathbf{X}^T \mathbf{X}} = 1 \quad (16)$$

Combining Equation 15 and Inequality 16, we can obtain:

$$\frac{\mathbf{X}^T ((1 - \alpha) \mathbf{N} - \mathbf{I}) \mathbf{X}}{\mathbf{X}^T \mathbf{X}} < (1 - \alpha) - 1 = -\alpha < 0$$

Therefore, 0 can't be the eigenvalue of $(1 - \alpha) \mathbf{N} - \mathbf{I}$. Then $(1 - \alpha) \mathbf{N} - \mathbf{I}$ is invertible.

Since **Lemma1.** holds, We can derive the concrete form of \mathbf{T} :

$$\mathbf{T} = \alpha ((1 - \alpha) \mathbf{N} - \mathbf{I})^{-1} \mathbf{H}$$

Thus we can keep recurring from equation 14 and obtain the following equation:

$$\mathbf{H}_k + \mathbf{T} = ((1 - \alpha) \mathbf{N})^k (\mathbf{H} + \mathbf{T}), \quad (17)$$

which also can be written as:

$$\mathbf{H}_k = ((1 - \alpha) \mathbf{N})^k \mathbf{H} + ((1 - \alpha) \mathbf{N})^k \mathbf{T} - \mathbf{T}. \quad (18)$$

For the second and third term in Eq.18, We write $(1 - \alpha) \mathbf{N}$ as $(1 - \alpha) \mathbf{N} - \mathbf{I} + \mathbf{I}$. Then We can use the binomial theorem to write $((1 - \alpha) \mathbf{N})^k$ as $\sum_{j=0}^k ((1 - \alpha) \mathbf{N} - \mathbf{I})^j$ then the Eq.18 can be written as :

$$\mathbf{H}_k = ((1 - \alpha) \mathbf{N})^k \mathbf{H} + \sum_{j=1}^k ((1 - \alpha) \mathbf{N} - \mathbf{I})^j \mathbf{T} \quad (19)$$

Bringing in the specific form of \mathbf{T} and further deriving the general formula of APPNP:

$$\begin{aligned} \mathbf{H}_k &= ((1 - \alpha) \mathbf{N})^k \mathbf{H} + \alpha \sum_{j=0}^{k-1} ((1 - \alpha) \mathbf{N} - \mathbf{I})^j \mathbf{H} \\ &= (1 - \alpha)^k \mathbf{N}^k \mathbf{H} + \alpha \sum_{j=0}^{k-1} \sum_{i=0}^j (-1)^{j-i} (1 - \alpha)^i \mathbf{N}^i \mathbf{H} \end{aligned}$$

□

□

A.3 Proof of theorem 3

To derive the general term formula of SDF-GCN, We need proof the following lemma first.

Lemma 2. Set all the diagonal element of Λ satisfy $0 < \lambda^{(i)} < 1$, then $(\Lambda \mathbf{N} + \mathbf{I})$ is invertible.

proof. To prove that $\Lambda \mathbf{N} + \mathbf{I}$ is invertible is equivalent to proving that its determinant are not equal to 0. Because all the diagonal element of Λ satisfy $0 < \lambda^{(i)} < 1$, then Λ is invertible, and due to

$$|\Lambda \mathbf{N} + \mathbf{I}| = |\Lambda| |\mathbf{N} + \Lambda^{-1}|. \quad (20)$$

Therefore, to prove that its determinant are not equal to 0 is equivalent to proving $|\mathbf{N} + \Lambda^{-1}|$ is not equal to 0, and further equivalent to proving $\mathbf{N} + \Lambda^{-1}$ does not have an eigenvalue of 0.

Consider the Rayleigh quotient of $\mathbf{N} + \Lambda^{-1}$:

$$\mathbf{R}_1 = \frac{\mathbf{X}^T (\mathbf{N} + \Lambda^{-1}) \mathbf{X}}{\mathbf{X}^T \mathbf{X}} \quad (21)$$

Split equation 20 , we derive:

$$\mathbf{R}_1 = \frac{\mathbf{X}^T \mathbf{N} \mathbf{X}}{\mathbf{X}^T \mathbf{X}} + \frac{\mathbf{X}^T \Lambda^{-1} \mathbf{X}}{\mathbf{X}^T \mathbf{X}} \quad (22)$$

The second term of Equation 21 can be easily written as follows:

$$\frac{\mathbf{X}^T \Lambda^{-1} \mathbf{X}}{\mathbf{X}^T \mathbf{X}} = \frac{\sum_{i=1}^N \lambda_i^{-1} x_i^2}{\sum_{i=1}^N x_i^2}. \quad (23)$$

Since $0 < \lambda_i < 1$, therefore , $\lambda_i^{-1} > 1$, so

$$\frac{\mathbf{X}^T \Lambda^{-1} \mathbf{X}}{\mathbf{X}^T \mathbf{X}} > 1. \quad (24)$$

For the first item, we write its specific form as follows:

$$\frac{\mathbf{X}^T \mathbf{N} \mathbf{X}}{\mathbf{X}^T \mathbf{X}} = \frac{\mathbf{X}^T (\tilde{\mathbf{D}}^{-\frac{1}{2}} \tilde{\mathbf{A}} \tilde{\mathbf{D}}^{-\frac{1}{2}}) \mathbf{X}}{\mathbf{X}^T \mathbf{X}} \quad (25)$$

From spectral graph theory we know that the following formula holds:

$$\mathbf{X}^T (\tilde{\mathbf{D}}^{-\frac{1}{2}} (\mathbf{A} + \mathbf{D}) \tilde{\mathbf{D}}^{-\frac{1}{2}}) \mathbf{X} = \sum_{(v_i, v_j) \in \mathcal{E}} \left(\frac{\mathbf{x}_i}{\sqrt{d_i + 1}} + \frac{\mathbf{x}_j}{\sqrt{d_j + 1}} \right)^2 > 0 \quad (26)$$

Further mathematically transforming this formula, we can get the following form:

$$\begin{aligned} \frac{\mathbf{X}^T (\tilde{\mathbf{D}}^{-\frac{1}{2}} (\mathbf{A} + \mathbf{D}) \tilde{\mathbf{D}}^{-\frac{1}{2}}) \mathbf{X}}{\mathbf{X}^T \mathbf{X}} &= \frac{\mathbf{X}^T (\tilde{\mathbf{D}}^{-\frac{1}{2}} (\tilde{\mathbf{A}} + \tilde{\mathbf{D}} - 2\mathbf{I}) \tilde{\mathbf{D}}^{-\frac{1}{2}}) \mathbf{X}}{\mathbf{X}^T \mathbf{X}} \\ &= \frac{\mathbf{X}^T (\tilde{\mathbf{D}}^{-\frac{1}{2}} \tilde{\mathbf{A}} \tilde{\mathbf{D}}^{-\frac{1}{2}}) \mathbf{X}}{\mathbf{X}^T \mathbf{X}} + \frac{\mathbf{X}^T (\tilde{\mathbf{D}}^{-\frac{1}{2}} \tilde{\mathbf{D}} \tilde{\mathbf{D}}^{-\frac{1}{2}}) \mathbf{X}}{\mathbf{X}^T \mathbf{X}} - \frac{2\mathbf{X}^T \tilde{\mathbf{D}}^{-1} \mathbf{X}}{\mathbf{X}^T \mathbf{X}} \\ &= \frac{\mathbf{X}^T (\tilde{\mathbf{D}}^{-\frac{1}{2}} \tilde{\mathbf{A}} \tilde{\mathbf{D}}^{-\frac{1}{2}}) \mathbf{X}}{\mathbf{X}^T \mathbf{X}} + 1 - \frac{2\mathbf{X}^T \tilde{\mathbf{D}}^{-1} \mathbf{X}}{\mathbf{X}^T \mathbf{X}} > 0 \end{aligned}$$

Further we get the following result:

$$\frac{\mathbf{X}^T (\tilde{\mathbf{D}}^{-\frac{1}{2}} \tilde{\mathbf{A}} \tilde{\mathbf{D}}^{-\frac{1}{2}}) \mathbf{X}}{\mathbf{X}^T \mathbf{X}} > \frac{2\mathbf{X}^T \tilde{\mathbf{D}}^{-1} \mathbf{X}}{\mathbf{X}^T \mathbf{X}} - 1 \quad (27)$$

It is trivial to have:

$$\frac{2\mathbf{X}^T \tilde{\mathbf{D}}^{-1} \mathbf{X}}{\mathbf{X}^T \mathbf{X}} = \frac{2 \sum_{i=1}^N (d_i + 1)^{-1} x_i^2}{\sum_{i=1}^N x_i^2} > 0 \quad (28)$$

Combining inequality 24, inequality 27 and inequality 28, we can get the following inequality:

$$\frac{\mathbf{X}^T (\tilde{\mathbf{D}}^{-\frac{1}{2}} \tilde{\mathbf{A}} \tilde{\mathbf{D}}^{-\frac{1}{2}} + \Lambda^{-1}) \mathbf{X}}{\mathbf{X}^T \mathbf{X}} > 0 \quad (29)$$

It can be obtained that the eigenvalue of $\tilde{\mathbf{D}}^{-\frac{1}{2}} \tilde{\mathbf{A}} \tilde{\mathbf{D}}^{-\frac{1}{2}} + \Lambda^{-1}$ is greater than 0, so 0 is not an eigenvalue of it. Further, $\Lambda \mathbf{N} + \mathbf{I}$ is invertible.

□

Now, we proof Theorem 1:

proof. Given the following recursive formula :

$$\mathbf{H}_k = \mathbf{H}_1 + \Lambda_{k-1} \left(\mathbf{H}_1 - \tilde{\mathbf{D}}^{-1/2} \tilde{\mathbf{A}} \tilde{\mathbf{D}}^{-1/2} \mathbf{H}_{k-1} \right) \quad (30)$$

where $\mathbf{H}_1 = \tilde{\mathbf{D}}^{-1/2} \tilde{\mathbf{A}} \tilde{\mathbf{D}}^{-1/2} \mathbf{H}$, $\Lambda_{k-1} = \text{diag}\{\lambda_{k-1}^{(1)}, \dots, \lambda_{k-1}^{(n)}\}$ $\lambda_i \sim \text{Sigmoid}(\mathcal{N}(\alpha_{k-1}^{(i)}, \beta_{k-1}^{(i)})^2)$.

After mathematical transformation, equation 30 can be written as

$$\mathbf{H}_k = (\mathbf{I} + \Lambda_{k-1}) \mathbf{H}_1 - \Lambda_{k-1} \tilde{\mathbf{D}}^{-1/2} \tilde{\mathbf{A}} \tilde{\mathbf{D}}^{-1/2} \mathbf{H}_{k-1}. \quad (31)$$

Set $\mathbf{N} = \tilde{\mathbf{D}}^{-1/2} \tilde{\mathbf{A}} \tilde{\mathbf{D}}^{-1/2}$ then equation 31 can be abbreviated as

$$\mathbf{H}_k = (\mathbf{I} + \Lambda_{k-1}) \mathbf{H}_1 - \Lambda_{k-1} \mathbf{N} \mathbf{H}_{k-1}. \quad (32)$$

We tried to modify Equation 32 to a form that more suitable for obtaining the general term :

$$\mathbf{H}_k + \mathbf{M}_{k-1} = -\Lambda_{k-1} \mathbf{N} (\mathbf{H}_{k-1} + \mathbf{M}_{k-1}). \quad (33)$$

In order to verify whether there exists such \mathbf{M} that satisfies the equation ,we need to solve the following equation:

$$-\Lambda_{k-1} \mathbf{N} \mathbf{M}_{k-1} = (\mathbf{I} + \Lambda_{k-1}) \mathbf{H}_1 + \mathbf{M}_{k-1} \quad (34)$$

which is equivalent to solving the equation :

$$-(\Lambda_{k-1} \mathbf{N} + \mathbf{I}) \mathbf{M}_{k-1} = (\mathbf{I} + \Lambda_{k-1}) \mathbf{H}_1. \quad (35)$$

Based on the definition , all the diagonal element of Λ_k satisfy $0 < \lambda_k^{(i)} < 1$, so according to Theorem 1, $(\Lambda_{k-1} \mathbf{N} + \mathbf{I})$ is invertible. Then $\mathbf{M}_{k-1} = -(\Lambda_{k-1} \mathbf{N} + \mathbf{I})^{-1} (\mathbf{I} + \Lambda_{k-1}) \mathbf{H}_1$ which means such \mathbf{M}_{k-1} that we required exists.

First we perform the following mathematical transformation on equation 33:

$$\mathbf{H}_k + \mathbf{M}_{k-1} = -\Lambda_{k-1} \mathbf{N} (\mathbf{H}_{k-1} + \mathbf{M}_{k-2} + \mathbf{M}_{k-1} - \mathbf{M}_{k-2}) \quad (36)$$

,

which can be split into the following form:

$$\mathbf{H}_k + \mathbf{M}_{k-1} = -\Lambda_{k-1} \mathbf{N} (\mathbf{H}_{k-1} + \mathbf{M}_{k-2}) + (-\Lambda_{k-1} \mathbf{N}) (\mathbf{M}_{k-1} - \mathbf{M}_{k-2}) \quad (37)$$

Let $\tilde{\mathbf{N}}_{k-1}$ denote $-\Lambda_{k-1} \mathbf{N}$,So the formula can be simply written as:

$$\mathbf{H}_k + \mathbf{M}_{k-1} = \tilde{\mathbf{N}}_{k-1} (\mathbf{H}_{k-1} + \mathbf{M}_{k-2}) + \tilde{\mathbf{N}}_{k-1} (\mathbf{M}_{k-1} - \mathbf{M}_{k-2}) \quad (38)$$

We first use equation 33 to recurse once, then derive the following formula:

$$\mathbf{H}_k + \mathbf{M}_{k-1} = \tilde{\mathbf{N}}_{k-1} \tilde{\mathbf{N}}_{k-2} (\mathbf{H}_{k-2} + \mathbf{M}_{k-2}) + \tilde{\mathbf{N}}_{k-1} (\mathbf{M}_{k-1} - \mathbf{M}_{k-2}) \quad (39)$$

By analogy, continuing to split and iterate, we can get the general term formula of the output of the k-th layer :

$$\mathbf{H}_k = \sum_{i=2}^{k-1} \prod_{j=i}^{k-1} \tilde{\mathbf{N}}_j (\mathbf{M}_i - \mathbf{M}_{i-1}) + \prod_{i=1}^{k-1} \tilde{\mathbf{N}}_i (\mathbf{H}_1 + \mathbf{M}_1) - \mathbf{M}_{k-1} \quad (40)$$

□

A.4 Experiment Setup

A.4.1 Dataset Statistics

The dataset statistics is shown in Table 4. Cora, Citeseer, and Pubmed were applied to all experiments, in addition to using the CoauthorCS and CoraFull datasets additionally for the SSNC experiments. For CoauthorCS and CoraFull, we randomly split all nodes into 0.5%/5%/94.5% for training/validation/testing. For the SSNC-MV experiments, we took the same experiments as [19, 20, 21], removing features from the validation and test sets of Cora, Citeseer, and Pubmed. The datasets are publicly available at: <https://github.com/dmlc/dgl/tree/master/python/dgl/data>

Table 4: Dataset Statistics.

	Cora	Citeseer	Pubmed	CoauthorCS	CoraFull
#Nodes	2708	3327	19717	18333	19793
#Edges	5429	4732	44338	81894	126842
#Features	1433	3703	500	6805	8710
#Classes	7	6	3	15	70
#Training Nodes	140	120	60	92	99
#Validation Nodes	500	500	500	917	990
#Testing Nodes	1000	1000	1000	17324	18704

A.4.2 Parameter Settings

Experiments in Section 3.2 We apply GCN,GAT with 32 hidden units .We fix the following sets of hyperparameters: dropout = 0.0,weight decay=0.0005.The learning rate is set to 0.01 if the number of layers is less than 16, and 0.001 if the number of layers is greater than or equal to 16.

Experiments in Section 5.2 We apply all the models with 64 hidden units on five datasets. We used the optimal parameters specified in the original papers for APPNP, GCNII and JKNet.For other models,we fix the following sets of hyperparameters: dropout=0.5,weight decay=0.0005,learning rate = 0.01.

Experiments in Section 5.3 We apply all the models with 64 hidden units.We fix the following sets of hyperparameters: dropout=0.5,weight decay=0.0005,learning rate = 0.01.The GCN equipped with the Res module is the GCNII.

Experiments in Section 5.4 We apply all the models with 32 hidden units.We fix the following sets of hyperparameters: dropout=0.5,weight decay=0.0005. The learning rate is set to 0.01 if the number of layers is less than 15, and 0.001 if the number of layers is greater than or equal to 15.

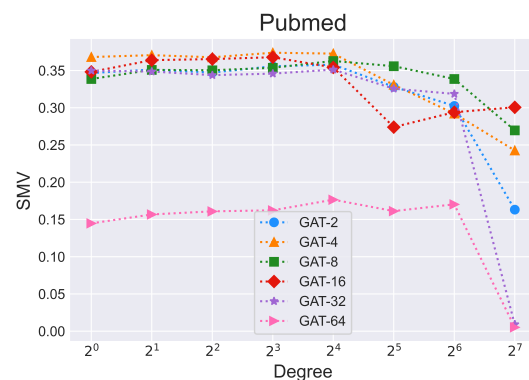
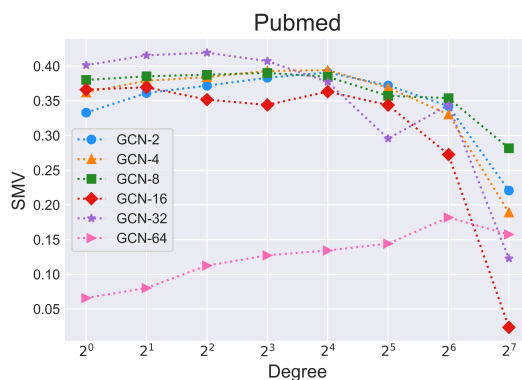
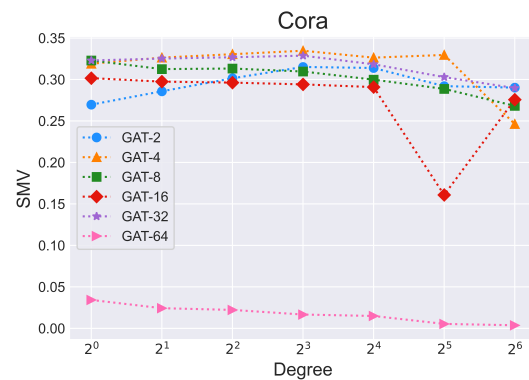
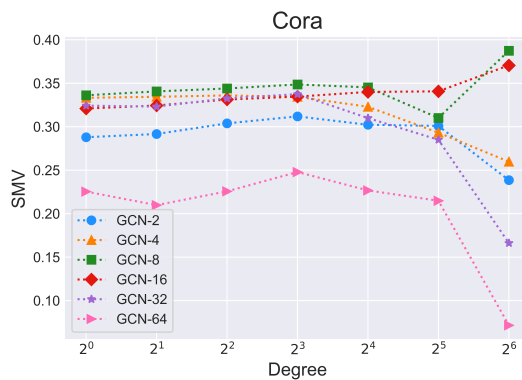
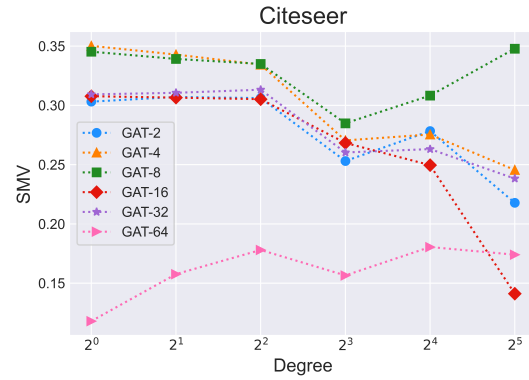
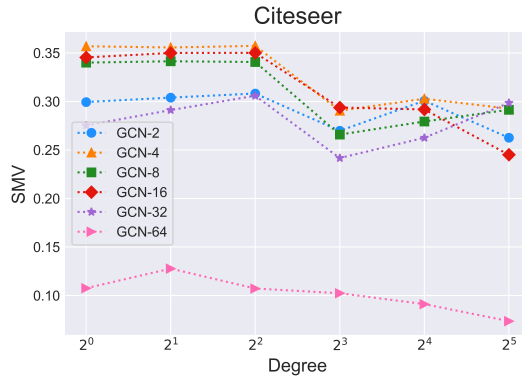
Experiments in Section 5.5 We apply all the models with 64 hidden units.We fix the following sets of hyperparameters: dropout=0.5,weight decay=0.0005.The learning rate is set to 0.01 if the number of layers is less than 16, and 0.001 if the number of layers is greater than or equal to 16.

A.4.3 Baselines

The baseline methods are publicly available at:

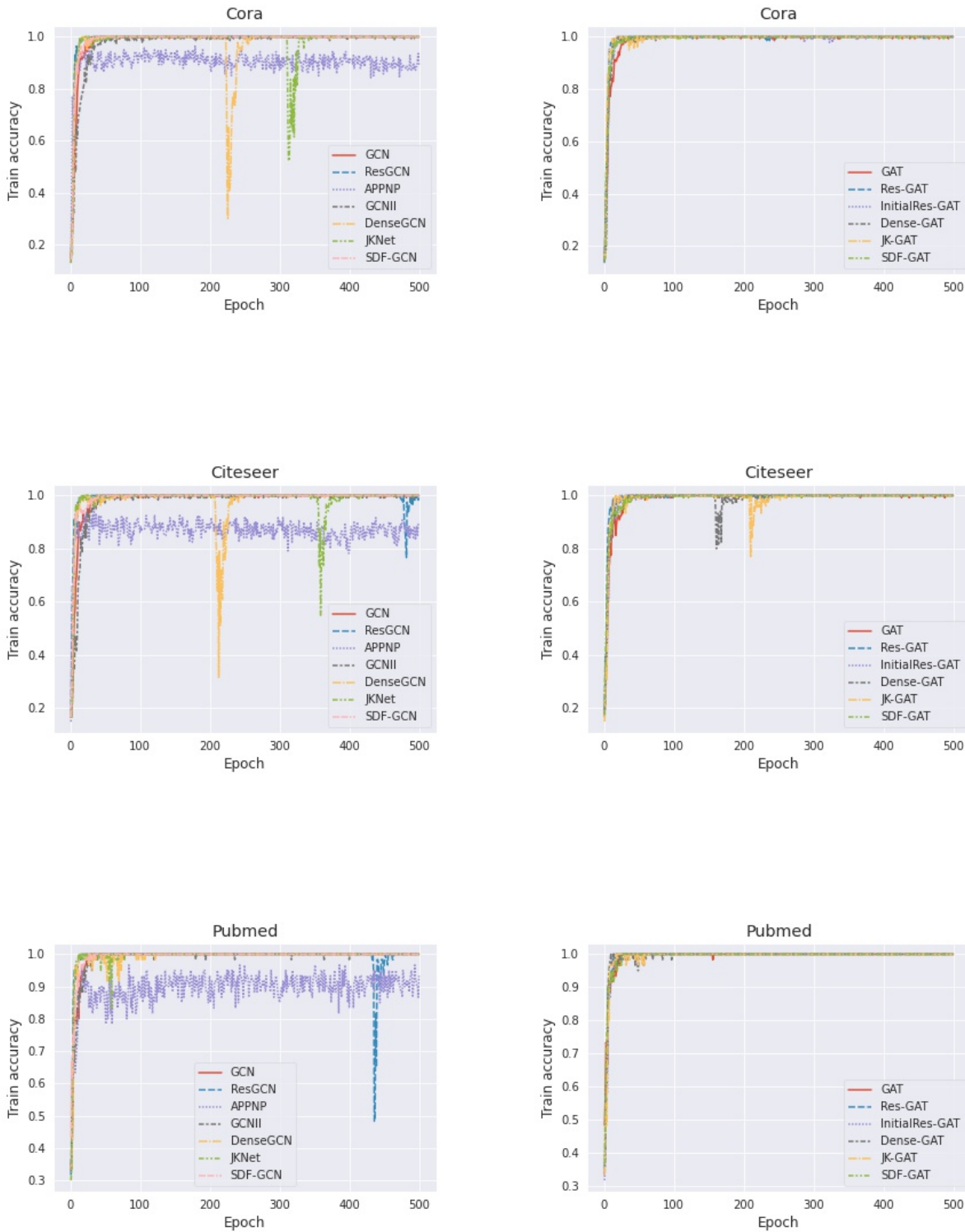
- **DGN,PairNorm,BatchNorm:** <https://github.com/Kaixiong-Zhou/DGN/>
- **DropEdge:**<https://github.com/DropEdge/DropEdge>
- **Other Models(APPNP,GCNII,...):**<https://github.com/JingboZhou-JLU/SDF-GNN>

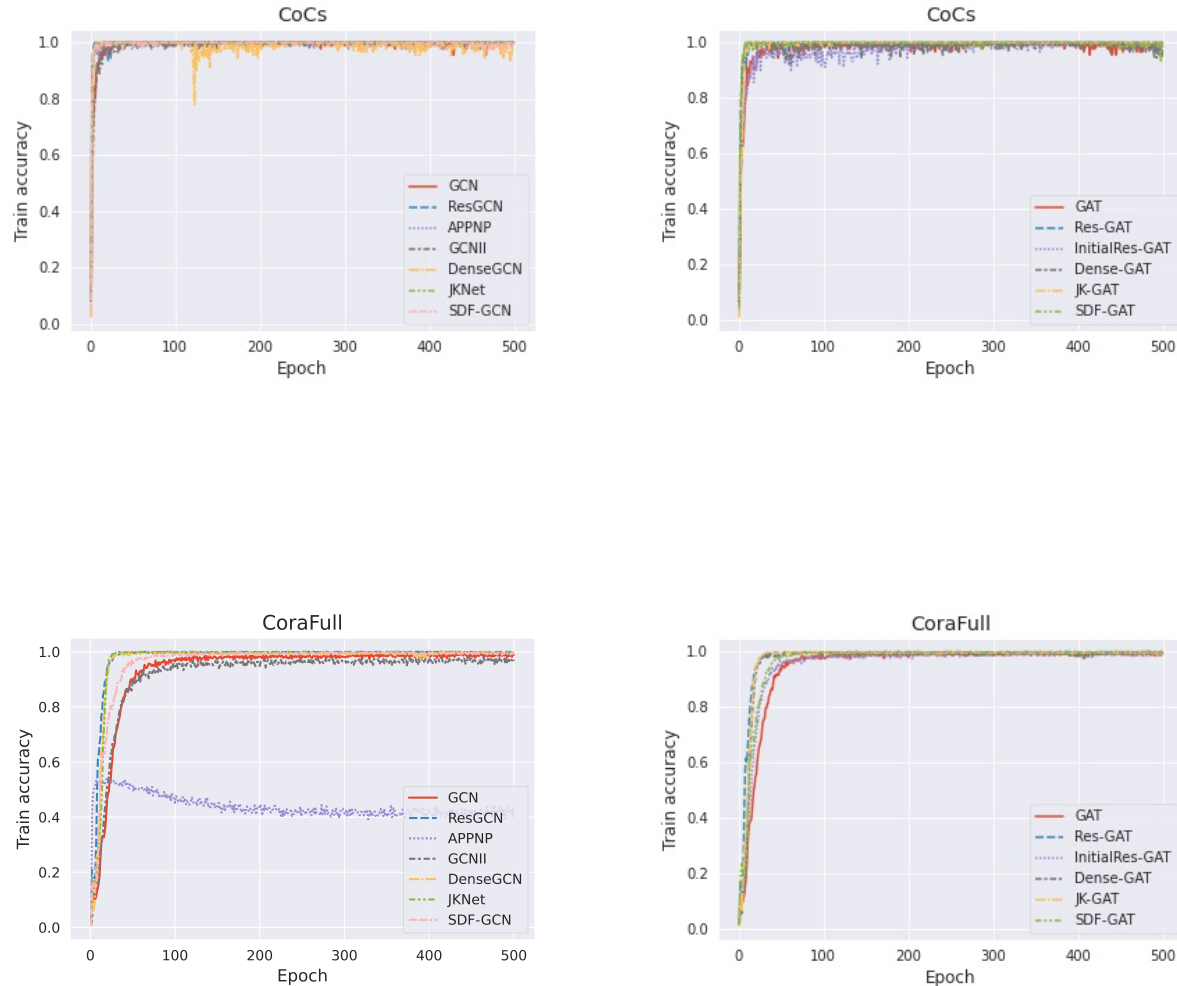
A.5 SMV of varying degrees nodes



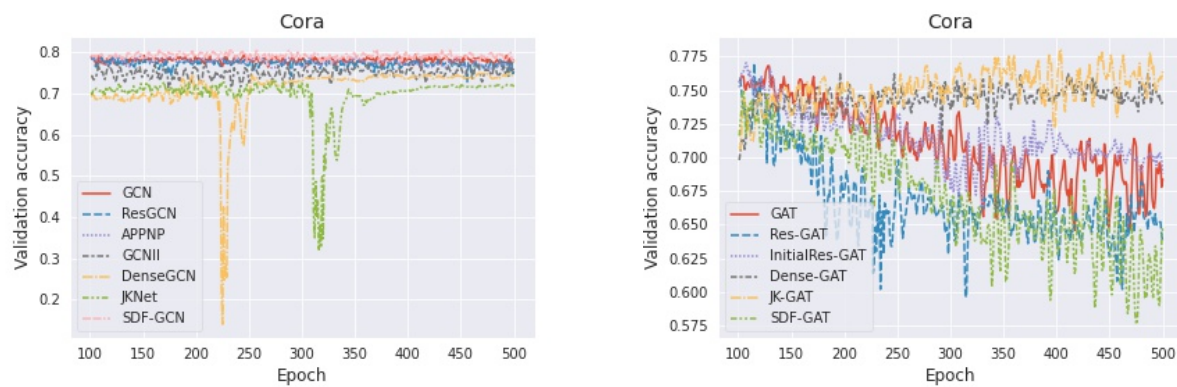
A.6 Overfitting Analysis of SSNC

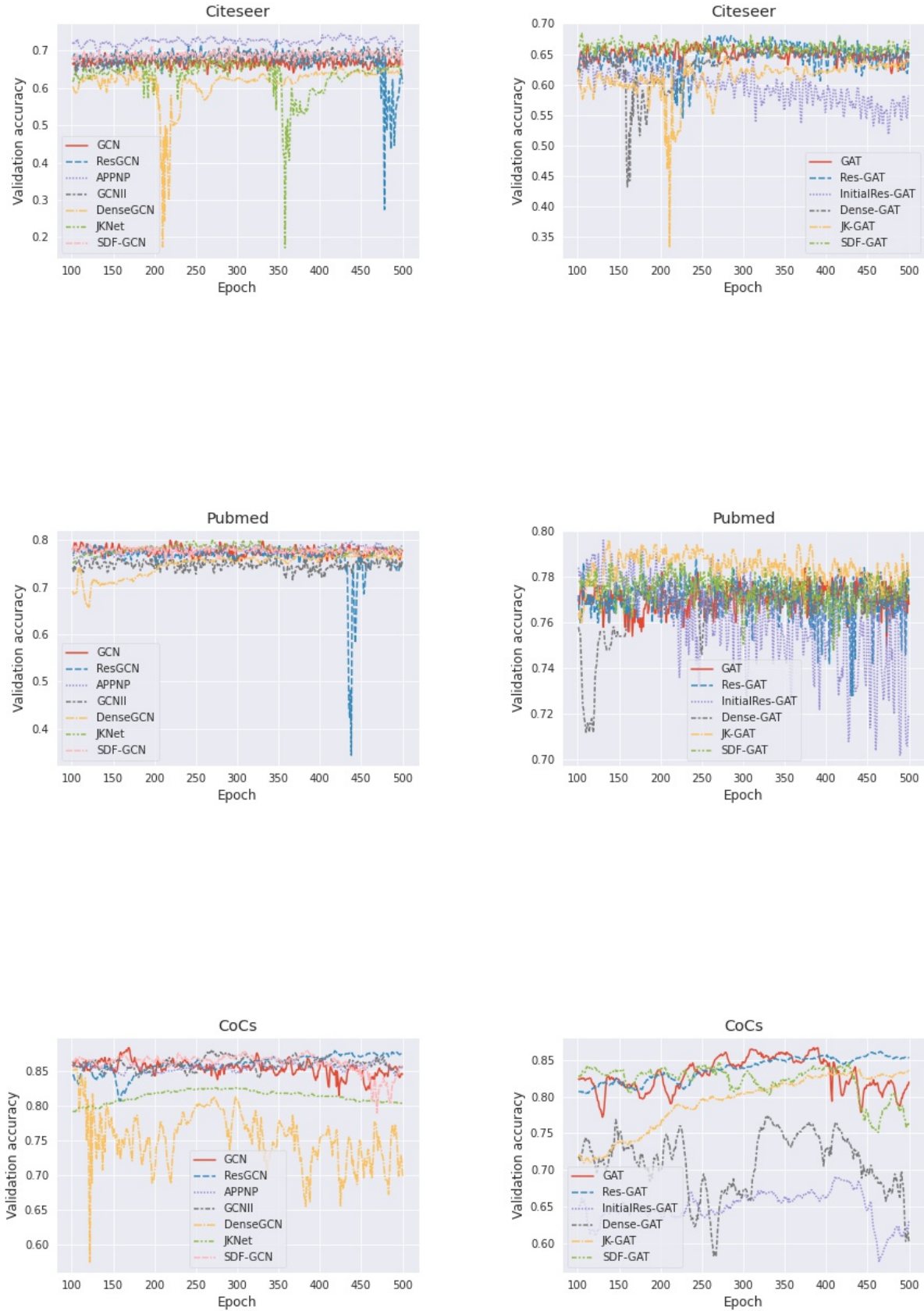
A.6.1 Train accuracy

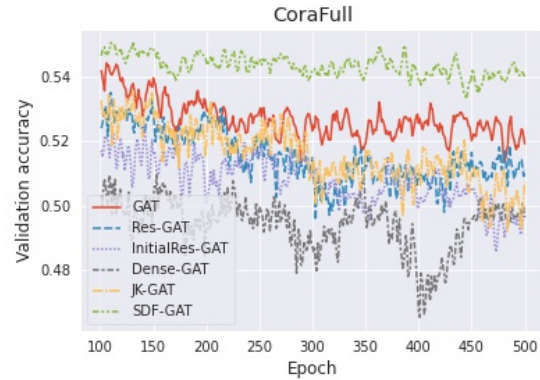
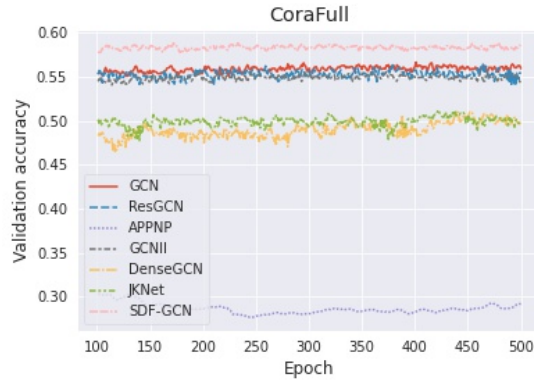




A.6.2 Validation accuracy







A.7 Efficiency Analysis

